IEEE Robotics and Automation Letters (RAL) paper presented at the
2020 IEEE/RSJ International Conference on Intelligent Robots and Systems (IROS)
October 25-29, 2020, Las Vegas, NV, USA (Virtual)

Open-Loop Orientation Control Using Dynamic Magnetic Fields

Andrew J. Petruska

***Abstract*— Remote magnetic control of soft magnetic objects has been limited to 2D orientation and 3D position. In this paper, we extend the five degree-of-freedom (5-DoF) control approach to full 6-DoF. We prove that 6-DoF control is possible for objects that have an apparent magnetic susceptibility tensor with unique eigenvalues. We further show that the object's orientation can be specified with a dynamic magnetic field and can be controlled without orientation feedback. The theory is demonstrated by rotating a soft magnetic object about each of its principle axes using a metronome like dynamic field.**

I. Introduction

Magnetic manipulation of an untethered object allows the control force and control torque to be applied without any mechanical contact between the object and the control system. For medical devices, this opens a new arena of minimally invasive techniques because a magnetic object inside the body, for example, can be manipulated by a system residing completely outside the body. Advances in the application of magnetic manipulation to medical tasks requires further advancements in the control of magnetic devices that overcome existing fundamental limitations. For example, full pose control, both orientation and position, is not currently practical for untethered magnetic devices. This limitation is a hindrance to the adoption of magnetic manipulation for medical applications. The rotation of a medically guided camera, for instance, would be uncontrolled.

Medical applications for magnetic manipulation have been explored since the 1700's [1], [2]. In spite of this long history, precise manipulation of a remote magnetic object was elusive until the 1980's when a small metal elliptical seed was magnetically guided for hyperthermic ablation of a tumor [3]. This system was constructed with six superconducting magnets and was incapable of full control of the seed [4], [5]. The first system capable of full control of a magnetic object was the OctoMag system [6], though only five degree of freedom (DoF) control, i.e. 3D position and 2D heading, was demonstrated. In this system, the heading was set in an open-loop fashion by the prevailing field direction, and the position was controlled using optical feedback.

The first demonstration of full 6-DoF control of a remote magnetic object was achieved by Berkelman et al. [7]. This approach leverages a device comprising several embedded permanent magnets. By independently applying a force and torque to each of these magnets, full orientation control of the composite system is achieved. A similar approach was demonstrated for micro-robotic applications by Diller et al. [8] and extended to single-body micro-robots by Giltinan et al. [9]. Unlike the 5-DoF control approaches previously demonstrated, these approaches use feedback to stabilize the full orientation of the object, leverage magnetic programming with permanent magnetic materials, and do not apply to soft-magnetic objects.

Andrew J. Petruska is with the M^{3}Robotics Lab, Colorado School of Mines, 1500 Illinois St, Golden, Colorado, USA 80401 apetruska@mines.edu

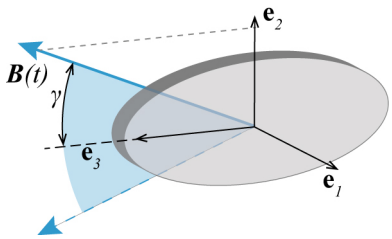

Fig. 1. A dynamic metronome-like field can stabilize the 3D orientation of a soft magnetic object. The magnetic field $\mathbf{B}(t)$ oscillates in a plane over some angle γ. The average field direction specifies the heading of the device, while the plane specifies the rotation about its heading.

Earnshaw's theorem states that the position of an untethered magnetic object in a magnetic field is unstable and requires feedback or nonmagnetic interactions for precision manipulation [10]. However, Earnshaw's theorem does not apply to object orientation, and open-loop control of the 3D orientation of an object remains a possibility. In this work, we show that a periodic field can induce a stable orientation and provide a methodology for assessing the orientation stability induced by other periodic field choices.

This paper is structured as follows. First, 5-DoF magnetic control is reviewed. Then, we prove that stable 3D orientation control can be achieved for soft magnetic objects using a dynamic field, shown in Fig. 1. Given these results, the optimal dynamic field and object properties are determined. Finally, we demonstrate this capability using the OctoMag system to perform 6-DoF object control without orientation feedback.

II. 5-DoF Manipulation

Before exploring how to stably generate 3D orientation control, it is beneficial to first review how 5-DoF control is achieved. Magnetic fields can generate a torque $\mathbf{T}$ on a magnetized body, which has a magnetic moment $\mathbf{m}$, and their spatial gradients can generate a force $\mathbf{F}$

$$\mathbf{T} = [\mathbf{m}]_\times \mathbf{B} \quad (1)$$

$$\mathbf{F} = \boldsymbol{\nabla}(\mathbf{m}\cdot\mathbf{B}), \quad (2)$$

where $[\mathbf{m}]_\times$ denotes the cross-product matrix packing of the vector $\mathbf{m}$. The force equation (2) can be restructured as

$$\begin{aligned}\mathbf{F} &= \begin{bmatrix} \mathrm{m_x} & \mathrm{m_y} & \mathrm{m_z} & 0 & 0 \\ 0 & \mathrm{m_x} & 0 & \mathrm{m_y} & \mathrm{m_z} \\ -\mathrm{m_z} & 0 & \mathrm{m_x} & -\mathrm{m_z} & \mathrm{m_y} \end{bmatrix} \begin{bmatrix} \frac{\partial \mathrm{B_x}}{\partial \mathrm{x}} \\ \frac{\partial \mathrm{B_x}}{\partial \mathrm{y}} \\ \frac{\partial \mathrm{B_x}}{\partial \mathrm{z}} \\ \frac{\partial \mathrm{B_y}}{\partial \mathrm{y}} \\ \frac{\partial \mathrm{B_y}}{\partial \mathrm{z}} \end{bmatrix} \\ &= \mathcal{F}(\mathbf{m})\,\mathbf{G}, \end{aligned} \tag{3}$$

where $\mathbf{G}$ is a vector packing of the five independent terms in the symmetric zero-trace field gradient tensor [5], [11].

Because the magnetic potential energy of a point dipole, $U = -\mathbf{m} \cdot \mathbf{B}$, is minimized when the field and the dipole moment are aligned, the heading of the object will align with the magnetic field direction. Thus, 5-DoF control is often implemented by specify a desired heading through the choice in field direction, and a desired force as required by a feedback control law. In this case, a field and force actuation matrix A_{BF} is used for control

$$\begin{aligned}\begin{bmatrix} \mathbf{B} \\ \mathbf{F} \end{bmatrix} &= \begin{bmatrix} \mathbb{I} & \mathbb{O} \\ \mathbb{O} & \mathcal{F}(\mathbf{m}) \end{bmatrix} \begin{bmatrix} \mathbb{B}(\mathbf{p}) \\ \mathbb{G}(\mathbf{p}) \end{bmatrix} \mathbf{I} \\ &= A_{BF}(\mathbf{m}, \mathbf{p})\,\mathbf{I}, \end{aligned} \tag{4}$$

where $\mathbb{I}$ indicates an appropriately sized identity matrix, $\mathbb{O}$ is an appropriated sized zero matrix, $\mathbb{B}$ is a sensitivity matrix relating field and current, $\mathbb{G}$ is a sensitivity matrix relating $\mathbf{G}$ and current, $\mathbf{I}$ is a vector-packing of the electromagnets' currents, and $\mathbf{p}$ is the objects position. In either case, the system must be over-actuated for there to be no orientation-dependent singularities [5]. Thus, the currents are chosen using a pseudoinverse, such as the Moore-Penrose inverse which minimizes the 2-norm of the currents required [12]. Furthermore, a minimum power solution can be derived that accounts for the semi-arbitrary choice of magnetic field strength [4], [13]. Permanent magnet systems capable of 5-DoF manipulation, e.g. [14], [15], can also be used to implement the following approach, albeit with a different input-to-field mapping [11].

III. Achieving the 6TH DoF

Soft magnetic objects magnetize linearly with the applied field when not near their saturation region. Solving for the nonuniform magnetization of a general soft magnetic body in a nonuniform field is best left to finite element analysis. However for control purposes, it is often assumed that the object is isotropic, has no remanence, and is small enough that it magnetizes as if it were in a uniform field, i.e.

$$\mathbf{m} = \frac{1}{\mu_0} R \left(\frac{1}{\chi_m} \mathbb{I} + N \right)^{-1} R^\top \mathbf{B} = X\mathbf{B} \tag{5}$$

where χ_m is the material's intrinsic magnetic susceptibility, N is the object's diagonal demagnetization tensor, and R is a rotation matrix that maps the object's principle magnetic coordinate frame to the world frame [16]. The matrix X is the apparent susceptibility tensor. For small applied fields, X is a function of the object's geometry, material properties, and rotation between the magnetic field frame and the object's principle frame. The principal eigenvector of X is referred to as the magnetic easy-axis, because this is the direction along which the device is most easily magnetized. Combining (1) and (5), the torque experienced by a soft magnetic body is quadratic in field, i.e.

$$\mathbf{T} = -[\mathbf{B}]_\times X\mathbf{B}. \tag{6}$$

If X has all unique eigenvalues, torque can be applied about any axis. If X has two unique eigenvalues, torque can only be applied about two axes [17]. If X has all equal eigenvalues, e.g. a sphere, no torque can be applied.

Although the magnetic torque is quadratic, the necessary field can be solved for directly by noting that both the magnetization and the field will be orthogonal to the torque. Thus, the required field direction can be extracted from a null space

$$\hat{\mathbf{B}} = \mathrm{null}\left(\begin{bmatrix} \mathbf{T}_{des}^\top X \\ \mathbf{T}_{des}^\top \end{bmatrix} \right) \tag{7}$$

and the magnitude is then

$$\|\mathbf{B}\| = \pm \frac{\|\mathbf{T}_{des}\|}{\left\| \left[\hat{\mathbf{B}}\right]_\times X\hat{\mathbf{B}} \right\|}, \tag{8}$$

where the hat operator $\hat{\cdot}$ indicates a unit vector.

This method provides a means to control the 3D orientation of a soft magnetic object, but it requires the tracking of the object's full orientation. It is well known that if a soft magnetic object is free to rotate and placed in a constant magnetic field, then the magnetic easy-axis will align with the applied field, like a compass needle. As discussed, this rotational stability has been exploited by 5-DoF control approaches that do not require any orientation information. A similar approach is desirable for 6-DoF control, but it will require a dynamic field.

Orientation free 5-DoF control uses quasi-static magnetic fields to specify the heading of the device, but rotations of the device about this heading remain uncontrolled. This approach degrades as the desired rotational rate of the object increases, because the torque required to rotate the object comes from a misalignment between the magnetic easy-axis and the applied field. Once the misalignment reaches 45º for soft magnetic objects, the maximum rotational rate is reached [17]. This phenomenon is referred to as step-out in the magnetic swimmer literature [18], [19]. At frequencies much higher than step-out, the magnetic object cannot follow the field and becomes effectively stationary due to the low-pass filtering of the mechanical system. We exploit this effect to specify the full orientation of the object.

Let the dynamic field at the object be $\mathbf{B}(t)$, and assume it oscillates at some periodicity τ that is short enough so that the orientation of the magnetic object is effectively constant. Without loss of generality, let $\mathbf{B}(t)$ be expressed in the magnetic object's principle magnetic coordinate system such that R in (5) is the identity matrix and X is diagonal

$$X = \mathrm{diag}(\chi_1, \chi_2, \chi_3). \tag{9}$$

Furthermore, we assume the object's magnetic easy-axis corresponds to the $\mathbf{e}_3$ direction and the object's minor axis corresponds to the $\mathbf{e}_1$ direction, as depicted in Fig. 1. The average torque over one period is, thus,

$$\bar{\mathbf{T}} = \frac{1}{\tau}\int_0^\tau \begin{bmatrix} -(\chi_3-\chi_2)B_2B_3 \\ (\chi_3-\chi_1)B_1B_3 \\ -(\chi_2-\chi_1)B_1B_2 \end{bmatrix} dt, \tag{10}$$

where the operator $\bar{\cdot}$ indicates a average over one period. Inspection of (10) shows, the magnetic susceptibilities need to be unique for any torque to be produced. Moreover, since $\mathbf{B}(t)$ has a single period τ, the average torque is nonzero only if the field variation in two directions is in phase and the product, for example B_2B_3, is an even function.

There are many dynamic fields that can satisfy this requirement. Here we propose a natural choice: a field that oscillates like a mechanical metronome. Note: this intuitive choice may be suboptimal. The resulting field depicted in Fig. 1, is given by

$$\mathbf{B} = B\begin{bmatrix} 0 \\ \sin\left(\gamma\sin\left(\frac{1}{\tau}t\right)\right) \\ \cos\left(\gamma\sin\left(\frac{1}{\tau}t\right)\right) \end{bmatrix}, \tag{11}$$

where B is the magnitude of the field and the metronome sweep angle γ is restricted to to the range $[0,\pi]$ for practicality and discussion clarity, although the analysis could be extended to any γ. The time average of this field is

$$\bar{\mathbf{B}} = J_0(\gamma)B\mathbf{e}_3, \tag{12}$$

where $J_0(\cdot)$ is the zero$^{\text{th}}$ order Bessel function of the first kind and B is the desired field magnitude. Integrating (10) with this field choice results in zero net torque. Thus, this is an equilibrium orientation if the frequency $1/\tau$ is much faster than the object's step-out frequency. The average torque induced from slight orientation perturbations determines if this is a stable equilibrium.

Without loss of generality, the orientation of the object R will be parametrized using an angle-axis representation

$$R = e^{[\mathbf{\Omega}]_\times}, \tag{13}$$

where the vector $\mathbf{\Omega}$ defines a rotation axis and has a length, in radians, quantifying the rotation amount [20]. The derivative of a rotated vector with this parametrization is given in [21] and the derivative of the torque with respect to object orientation becomes

$$\frac{\partial\mathbf{T}}{\partial\Omega} = [\mathbf{B}]_\times\left([X\mathbf{B}]_\times - X[\mathbf{B}]_\times\right). \tag{14}$$

Given the dynamic field (11), the average torque derivative is a diagonal matrix with entries

$$\frac{1}{\tau}\int_0^\tau \frac{\partial\mathbf{T}}{\partial\mathbf{\Omega}}d\tau = \text{diag}\begin{pmatrix} (\chi_2-\chi_3)J_0(2\gamma)B^2 \\ \frac{(\chi_1-\chi_3)}{2}(J_0(2\gamma)+1)B^2 \\ \frac{(\chi_1-\chi_2)}{2}(1-J_0(2\gamma))B^2 \end{pmatrix}. \tag{15}$$

A plot of the Bessel terms is provided in Fig. 2 for $0 \le \gamma \le \pi$. For the object to be in a stable dynamic equilibrium, these terms must be negative. The middle term

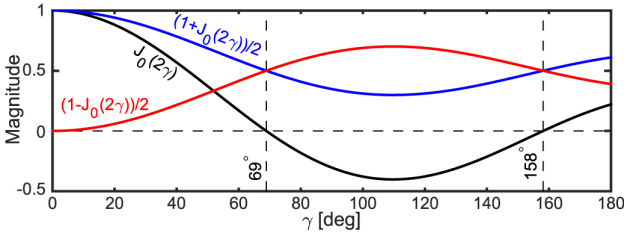

Fig. 2. Average torque derivative Bessel function contributions plotted from $0 \le \gamma \le \pi$, and scaled to degrees for readability. The sign change in $J_0(2\gamma)$ indicates that the object's major axis changes from being parallel to the average field, for low and high values of γ, to being orthogonal to the average field, for intermediate values of γ.

$((J_0(2\gamma)+1)/2)$ is always negative as long as $\chi_3 > \chi_1$ and the last term $((1-J_0(2\gamma))/2)$ is negative if $\chi_2 > \chi_1$. As expected, when $\gamma = 0$, the last term, which corresponds to the average torque derivative for rotations about the magnetic easy-axis, is zero. For both small ($\gamma < 0.38\pi$) and large ($\gamma > 0.88\pi$) metronome angles, the first term ($J_0(2\gamma)$) is negative when $\chi_3 > \chi_2$. However, at intermediate angles, i.e. $0.38\pi \le \gamma \le 0.88\pi$ ($69° \le \gamma \le 158°$), $J_0(2\gamma)$ is negative and an alignment between the magnetic easy-axis and the average field is not stable. A rotation of the object about its $\mathbf{e}_1$ axis by $\pi/2$ will interchange the χ_2 and χ_3 terms in (15) and make the orientation stable. To summarize, in the dynamic field the object will align such that its minor magnetic axis is orthogonal to the plane swept out by the magnetic field for any $\gamma \neq 0$. Furthermore, the object's major axis will align parallel to the average field if $\gamma < 0.38\pi$ or $\gamma > 0.88\pi$, but it will align orthogonal to the applied field direction if $0.38\pi \le \gamma \le 0.88\pi$. Therefore, given a short enough τ, an appropriate γ, and unique values of χ_1, χ_2, and χ_3, the full orientation of the object is stably constrained by the dynamic field.

The actual restoring torques are a function of the shape anisotropy of the object. Clearly, some objects will perform better than others. For best performance, the object should have χ_1 as small as possible to maximize the restoring torque about the $\mathbf{e}_3$ axis. The optimal geometry and field oscillation angle combination satisfy

$$\begin{aligned} \underset{\chi_1,\chi_2,\chi_3,\gamma}{\text{argmin}} \quad & \max\left\{\begin{array}{l} \frac{(\chi_2-\chi_3)}{\max(\chi_2,\chi_3)}J_0(2\gamma) \\ \frac{(\chi_1-\chi_3)}{2\max(\chi_2,\chi_3)}(J_0(2\gamma)+1) \\ \frac{(\chi_1-\chi_2)}{2\max(\chi_2,\chi_3)}(1-J_0(2\gamma)) \end{array}\right\}, \\ \text{subject to} \quad & \left\{0 \le \chi_1, \quad \chi_1 \le \chi_2, \quad \chi_1 \le \chi_3 \right. \end{aligned} \tag{16}$$

where the $\max(\chi_2,\chi_3)$ term both normalizes the torque magnitude by the maximum susceptibility and accounts for the case when a $\pi/2$ rotation of the object is required to stabilize its orientation. Solving this problem numerically, the optimal parameter ratios are $\chi_1/\chi_3 = 0$, $\chi_2/\chi_3 = 0.586$, and $\gamma = 0.266\pi$ (47.9°) or $\chi_1/\chi_3 = 0$, $\chi_2/\chi_3 = 1.747$, and $\gamma = 0.594\pi$ (106.9°). The former optimum is the global optimum, but the difference is negligible. Figure 3 shows the optimal function values calculated by (16) at fixed γ and shows these two local optimum. At these optimum, the ratio

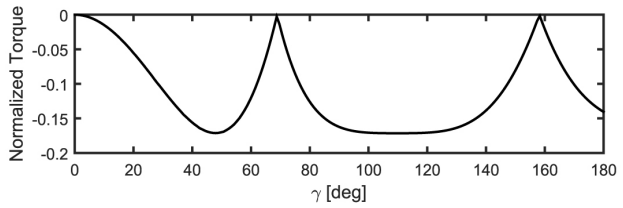

Fig. 3. Optimal worst-case restoring torque, which is optimized by (16), at fixed γ. There is a local optimum that occurs at χ_2/χ_3 = 0.586 and $\gamma = 0.266\pi$ (47.9°), which is only slightly better than the optimum that occurs at χ_2/χ_3 = 1.747 and $\gamma = 0.594\pi$ (106.9°). The later optimum corresponds to a configuration that aligns the object's magnetic easy-axis orthogonal to the average field direction.

of the maximum restoring-torque stiffness to the minimum restoring-torque stiffness S_r is

$$S_r = \frac{\chi_3}{\chi_2}\frac{J_0\left(2\gamma\right)+1)}{1-J_0\left(2\gamma\right)} \approx 4.1.$$

For a given object with three unique apparent magnetic susceptibilities, a dynamic field can be generated that stabilizes a desired orientation. Moreover, quasi-static adjustments to the dynamic field, i.e. changes at frequencies much less than the object's step-out frequency, will twist the object along with the coordinate system defined by the dynamic field. The control update for a magnetic manipulation system, given a desired control force $\mathbf{F}_{des}$ and desired orientation, which defines the susceptibility tensor X and is stabilized by $\mathbf{B}\left(t\right)$, becomes

$$\mathbf{I} = A_{BF}\left(X\mathbf{B}\left(t\right),\mathbf{p}\right)^{\dagger}\begin{bmatrix}\mathbf{B}\left(t\right)\\ \mathbf{F}_{des}\end{bmatrix}. \tag{17}$$

N.B., it is assumed X quasi-statically changes with the object's desired orientation, but $\mathbf{B}\left(t\right)$ changes rapidly in time. To implement this, it is important that the electrical current induced in the solenoids is able to track the desired dynamic field. Thus, both the control update rate and the magnetic manipulation system dynamics must be faster than $\mathbf{B}\left(t\right)$'s Nyquist frequency.

IV. Experimental Validation

All experiments were performed using the OctoMag system described in [6]. The object was tracked using two orthogonal cameras with a 30 Hz update rate. The soft magnetic elliptical cylinder measured 3.0x1.2x0.03 mm and was laser cut from 50-50 NiFe, which has a large χ_m and negligible magnetic remanence. Approximating the elliptical cylinder as an ellipsoid, the three susceptibility factors (χ_1, χ_2, χ_3) are respectively 1, 52, and 211 [22]. Solving (16) given the geometry's susceptibility, yields an optimal γ of 61° or 77°. With empirical tuning we found a γ of 80° had the best observed performance. The discrepancy could be due to human error in the tuning or errors between the susceptibilities calculated assuming an ellipsoid and the actual susceptibilities of the epileptic cross-section cylinder used. Given this, the dynamic magnetic field used to control the orientation of the object has a magnitude of 20 mT and

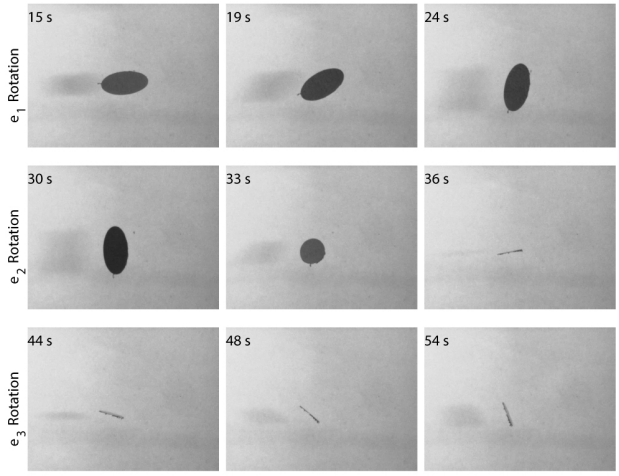

Fig. 4. A soft magnetic elliptical cylinder is rotated about each of its three axes by a metronome field applied at 10 Hz and γ of 80°. The rotation rate about $\mathbf{e}_3$ is $4^{\circ}/s$ for this setup.

sweeps out an angle of ±80º from its mean value at a frequency of 10 Hz. Because $0.38\pi \leq \gamma \leq 0.88\pi$, the $\mathbf{e}_2$ axis will align with the average field direction. The object's rotation about all three principle axis are shown in Fig 4 and in the multimedia attachment. Note that although the sweep angle and geometry are not optimal, the object is still capable of tracking the desired orientation. The maximum rotational rate about the magnetic easy axis that the object was able to track was 0.07 Hz (˜4 °/s).

V. Discussion

These experimental trials demonstrate that periodic field trajectories can be used to stabilize the orientation of the magnetic object. However, this opens new questions relative to optimization. From a geometric perspective, the demagnetizing factors and the viscus drag coefficients are both a function of geometry and similarly contribute to the maximum rotation rate of the body. This suggests a coupled fluidic-magnetic optimization may be performed to maximize the drag-limited maximum rotation rate. Furthermore, the field trajectory could be further optimized to enable faster rotations using optimal control approaches. For example, a field that dwells at each half period could be more productive during active rotations by averaging to a larger net rotational torque. These studies and the effects of magnetic crystal anisotropy and remanence are left for future studies.

VI. Conclusions

The full 6-DoF control of a soft magnetic object has been presented and demonstrated. The method does not require tracking the object's orientation, as it utilizes a dynamic magnetic field to stabilize the open-loop control of orientation. A soft magnetic elliptical cylinder was levitated against gravity and rotations about the three principle axes was demonstrated. The maximum rotational rate about the long axis of the structure was limited (0.07 Hz), but the object

was capable of following the desired orientation trajectory without any orientation feedback.

ACKNOWLEDGEMENT

The author would like to thank Bradley J. Nelson for his valuable suggestions on the manuscript and allowing access to the OctoMag system for testing validation.

REFERENCES

[1] E. H. Frei, "Medical applications of magnetism," *Crit Rev Solid State Mat Sci*, vol. 1, no. 3, pp. 381–407, Sep 1970.

[2] G. T. Gillies, R. C. Ritter, W. C. Broaddus, M. S. Grady, M. A. Howard III, and R. G. McNeil, "Magnetic manipulation instrumentation for medical physics research," *Rev Sci Instrum*, vol. 65, no. 3, pp. 533–562, Mar 1994.

[3] M. S. Grady, M. A. Howard III, J. A. Molloy, R. C. Ritter, E. G. Quate, and G. T. Gillies, "Preliminary experimental investigation of invivo magnetic manipulation: Results and potential application in hyperthermia," *Med Phys*, vol. 16, no. 2, pp. 263–272, Mar 1989.

[4] D. C. Meeker, E. H. Maslen, R. C. Ritter, and F. M. Creighton, "Optimal realization of arbitrary forces in a magnetic stereotaxis system," *IEEE Trans Magn*, vol. 32, no. 2, pp. 320–328, Mar. 1996.

[5] A. J. Petruska and B. J. Nelson, "Minimum Bounds on the Number of Electromagnets Required for Remote Magnetic Manipulation," *IEEE Trans Robot*, vol. 31, no. 3, pp. 714–722, May 2015.

[6] M. P. Kummer, J. J. Abbott, B. E. Kratochvil, R. Borer, A. Sengul, and B. J. Nelson, "OctoMag: An electromagnetic system for 5-DOF wireless micromanipulation," *IEEE Trans Robot*, vol. 26, no. 6, pp. 1006–1017, Dec 2010.

[7] P. Berkelman and M. Dzadovsky, "Magnetic levitation over large translation and rotation ranges in all directions," *IEEE/ASME Trans Mechatron*, vol. 18, no. 1, pp. 44–52, Feb 2013.

[8] E. Diller, J. Giltinan, G. Z. Lum, Z. Ye, and M. Sitti, "Six-degree-of-freedom magnetic actuation for wireless microrobotics," *Int J Rob Res*, pp. 1–15, Jun 2015.

[20] R. M. Murray, Z. Li, and S. S. Sastry, *A Mathematical Introduction to Robotic Manipulation*. CRC Press, 1994.

[9] J. Giltinan and M. Sitti, "Simultaneous six-degree-of-freedom control of a single-body magnetic microrobot," *IEEE Rob. Automa. Lett.*, vol. 4, no. 2, pp. 508–514, 2019.

[10] S. Earnshaw, "On the nature of the molecular forces which regulate the constitution of the luminiferous ether," *Trans. Camb. Phil. Soc*, vol. 7, pp. 97–112, 1842.

[11] J. J. Abbott, E. Diller, and A. J. Petruska, "Magnetic methods in robotics," *Annu Rev Robot Cont Autom*, vol. 3, pp. 2.1–2.34, May 2020.

[12] R. A. Horn and C. R. Johnson, *Matrix Analysis, reprint ed.* Cambridge, UK: Cambridge University Press, 1985.

[13] A. Komaee and B. Shapiro, "Steering a ferromagnetic particle by optimal magnetic feedback control," *IEEE Trans Control Syst Technol*, vol. 20, no. 4, pp. 1011–1024, Jul 2012.

[14] A. W. Mahoney and J. J. Abbott, "Five-degree-of-freedom manipulation of an untethered magnetic device in fluid using a single permanent magnet with application in stomach capsule endoscopy," *Int. J. Robot. Res.*, vol. 35, no. 1–3, pp. 129–147, 2016.

[15] P. Ryan and E. Diller, "Magnetic actuation for full dexterity microrobotic control using rotating permanent magnets," *IEEE Trans. Robot.*, vol. 33, no. 6, pp. 1398–1409, 2017.

[16] R. C. O'Handley, *Modern Magnetic Materials*. Wiley-Interscience, 2000.

[17] J. J. Abbott, O. Ergeneman, M. P. Kummer, A. M. Hirt, and B. J. Nelson, "Modeling magnetic torque and force for controlled manipulation of soft-magnetic bodies," *IEEE Trans Robot*, vol. 23, no. 6, pp. 1247–1252, Dec 2007.

[18] K. Ishiyama, K. I. Arai, M. Sendoh, and A. Yamazaki, "Spiral-type micro-machine for medical applications," in *Proc. Int. Symp. Micromechatronics and Human Science*, 2000, pp. 65–69.

[19] A. W. Mahoney, N. D. Nelson, K. E. Peyer, B. J. Nelson, and J. J. Abbott, "Behavior of rotating magnetic microrobots above the step-out frequency with application to control of multi-microrobot systems," *App Phys Let*, vol. 104, no. 14, 2014.

[21] G. Gallego and A. Yezzi, "A compact formula for the derivative of a 3-d rotation in exponential coordinates," *J Math Imaging Vis*, pp. 1–7, Aug 2014.

[22] J. A. Osborn, "Demagnetizing factors of the general ellipsoid," *Phys. Rev.*, vol. 67, pp. 351–357, Jun. 1945.